

**NASA TECHNICAL
MEMORANDUM**



NASA TM X-3029

NASA TM X-3029

**CASE FILE
COPY**

**CROSSFLOW EFFECTS ON
IMPINGEMENT COOLING
OF A TURBINE VANE**

*by James W. Gauntner, Herbert J. Gladden,
Daniel J. Gauntner, and Frederick C. Yeh*

*Lewis Research Center
Cleveland, Ohio 44135*

1. Report No. NASA TM X-3029	2. Government Accession No.	3. Recipient's Catalog No.	
4. Title and Subtitle CROSSFLOW EFFECTS ON IMPINGEMENT COOLING OF A TURBINE VANE		5. Report Date March 1974	
		6. Performing Organization Code	
7. Author(s) James W. Gauntner, Herbert J. Gladden, Daniel J. Gauntner, and Frederick C. Yeh		8. Performing Organization Report No. E-7768	
		10. Work Unit No. 501-24	
9. Performing Organization Name and Address Lewis Research Center National Aeronautics and Space Administration Cleveland, Ohio 44135		11. Contract or Grant No.	
		13. Type of Report and Period Covered Technical Memorandum	
12. Sponsoring Agency Name and Address National Aeronautics and Space Administration Washington, D. C. 20546		14. Sponsoring Agency Code	
		15. Supplementary Notes	
16. Abstract An air-cooled turbine vane was tested in a four-vane cascade. Heat-transfer characteristics of the impingement cooled midchord region are reported. Experimental Nusselt numbers of six midchord locations are examined for the effect of crossflow and compared to those predicted by impingement correlations found in the literature.			
17. Key Words (Suggested by Author(s)) Impingement cooling Turbine vane Crossflow Heat transfer		18. Distribution Statement Unclassified - unlimited	
19. Security Classif. (of this report) Unclassified		20. Security Classif. (of this page) Unclassified	22. Price* \$2.75
		21. No. of Pages 20	Cat. 33

CROSSFLOW EFFECTS ON IMPINGEMENT COOLING OF A TURBINE VANE

by James W. Gauntner, Herbert J. Gladden, Daniel J. Gauntner,
and Frederick C. Yeh

Lewis Research Center

SUMMARY

The heat-transfer characteristics of the impingement cooled midchord region of an air cooled turbine vane were determined experimentally. The vane was tested in a cascade at an average combustion gas temperature of 1255 K (1800⁰ F) and a coolant inlet temperature of 290 K (60⁰ F). The experimental results obtained for the impingement cooled region of the vane are examined for the effect of crossflow and compared to impingement correlations found in the literature.

At the conditions considered it was found that a crossflow did not adversely affect the cooling of the midchord region of an impingement cooled turbine vane. Impingement cooling correlations found in the literature did not adequately predict the experimental coolant side Nusselt numbers. The experimental Nusselt numbers were correlated with Reynolds numbers based on both crossflow and the distance between the point in question and the farthest upstream jet.

INTRODUCTION

Impingement heat transfer in the midchord region of a turbine vane was investigated in a four-vane cascade. The purpose of the investigation was to determine the effect of crossflow on impingement cooling and to compare the data with correlations from the literature.

Impingement cooling in turbine vanes appears attractive because of the high heat-transfer coefficients obtainable. Also, from a fabrication standpoint, the jet holes can be incorporated in the insert of the airfoil with relative ease. However, in the design of vanes and blades complete agreement does not exist regarding which of the existing correlations in the literature should be used when predicting heat transfer from arrays of impinging jets and whether or not crossflow affects impingement heat transfer. Reference 1 reported the results of tests on a turbine rotor blade having both an impinge-

ment cooled leading edge and midchord region. No effect of crossflow on impinging-jet heat transfer was found in the midchord region of the blade. No attempt was made in the analysis of reference 1 to consider the effect of the temperature drop through the wall or the effect of chordwise conduction along the wall of the rotor blade.

The investigation described herein, which is for a turbine stator vane, considers both of these effects. Coolant side Nusselt numbers are calculated from the experimental data. Next, the data are examined to determine if crossflow from upstream jets affects the impingement heat transfer at downstream locations. The experimental Nusselt numbers are also compared with correlations found in the literature to determine which correlation should be used in the design of turbine vanes.

The vane was tested in a cascade at an average gas temperature of 1255 K (1800° F), a coolant inlet temperature of 290 K (60° F), a turbine inlet pressure of 31 newtons per square centimeter (45 psia), and midchord coolant- to gas-flow ratios to about 0.06.

APPARATUS

Cascade Description

The cascade consisted of a combustor section, a transition section, a test section, and an exhaust section. A description of this cascade is given in reference 2. The test section was a 23° annular sector of a vane row and contained four vanes and five flow channels. The central flow channel was formed by the suction surface of the second vane and pressure surface of the third vane. These two central vanes, referred to herein as vanes 2 and 3, were used as the test vanes. The two outer vanes in the cascade complete the flow channels for the test vanes. They also served as radiation shields between the test vanes and the water cooled cascade walls.

Vane Description

A J-75 size vane, having a span of 9.78 centimeters (3.85 in.) and a chord of 6.28 centimeters (2.47 in.), was used in this investigation. The external profile is described in reference 3. The internal cooling configuration (see figs. 1 and 2) consisted of an impingement cooled midchord region and a pin fin augmented convection cooled trailing edge region. This vane was designed to have an impingement cooled leading edge. However, for this investigation, the leading edge impingement tube was removed and the chamber blocked at the tip end. Therefore, the cooling air entering the vane from the tip plenum was restricted to cooling the midchord and trailing edge regions only. The leading edge was uncooled.

The midchord supply tube contained a staggered array of 0.038-centimeter- (0.015-in.-) diameter holes. There were 481 and 334 holes, respectively, on the suction and pressure surfaces. The chordwise center-to-center hole spacing was 0.24 and 0.28 centimeter (0.095 and 0.110 in.) and the spanwise row spacing was 0.20 and 0.23 centimeter (0.080 and 0.092 in.), respectively, on the suction and pressure surfaces. The hole to target spacing was 0.076 centimeter (0.030 in.) or two hole diameters.

The split trailing edge contained four rows of oblong pin fins and a single row of round pin fins. The oblong pins were 0.38 centimeter (0.15 in.) by 0.25 centimeter (0.10 in.) and varied in height from 0.18 centimeter (0.070 in.) to 0.094 centimeter (0.37 in.). The round pins had a diameter of 0.20 centimeter (0.080 in.) and a height of 0.064 centimeter (0.025 in.).

INSTRUMENTATION

Fifteen Chromel-Alumel thermocouples were located at the vane midspan (see fig. 1). The exact locations of the thermocouples are given in table I. Because the gas inlet temperature was measured upstream at the central flow channel of the cascade, only the vane surfaces forming this flow channel were instrumented. Consequently, eight thermocouples were located on the suction surface of vane 2 and seven thermocouples were located on the pressure surface of vane 3. The construction and installation of the thermocouples is discussed in reference 4. Separate cooling air systems supplied each of the test vanes through turbine-type flowmeters. Cooling air temperature and pressure were measured at the inlet to the vanes. Combustion gas inlet conditions were measured by spanwise traversing probes. This instrumentation is discussed in reference 2.

ANALYSIS METHODS

A two-dimensional heat balance can be written for an element in the vane wall accounting for conduction both along the wall and through the wall. If the chordwise temperature gradient is assumed to be constant across the vane wall, the following equation can be written:

$$h_g(T_{ge} - T_{w,o}) = h_c(T_{w,i} - T_c) - tk_w \frac{d^2 T_w}{dx^2} \quad (1)$$

(Symbols are defined in the appendix.) If the local effective gas temperature and coolant temperature are replaced by the gas inlet and the coolant inlet temperatures, respectively, the solution of equation (1) for the coolant side heat-transfer coefficient yields equation (2).

$$h_c = h_g \frac{T_g - T_{w,o}}{T_{w,i} - T_{ci}} + \frac{k_w t}{T_{w,i} - T_{ci}} \frac{d^2 T_w}{dx^2} \quad (2)$$

In this equation the coolant side wall temperature $T_{w,i}$, the gas side heat-transfer coefficient h_g , and the thermal conductivity of the wall k_w are unknown. Let the temperature drop across the wall be approximated as follows:

$$\frac{k_w}{t} (T_{w,o} - T_{w,i}) = h_g (T_g - T_{w,o}) \quad (3)$$

If equation (3) is solved for the inside wall temperature and substituted into equation (2), the following equation results:

$$h_c = \left[h_g \left(\frac{T_g - T_{w,o}}{T_{w,o} - T_{ci}} \right) \right] \left[1 + \frac{k_w t}{h_g (T_g - T_{w,o})} \frac{d^2 T_w}{dx^2} \right] \left[1 - \frac{h_g}{k_w} \left(\frac{T_g - T_{w,o}}{T_{w,o} - T_{ci}} \right) \right]^{-1} \quad (4)$$

The first term on the right side is the uncorrected value for the coolant side heat-transfer coefficient. The second term is the correction for chordwise conduction, while the third term is the correction for the temperature drop across the vane wall. The second derivative of the wall temperature with respect to vane chord surface is obtained by numerically differentiating the experimental data at the point of interest.

The gas side heat-transfer coefficient for both turbulent and transitional boundary layers is calculated by the formulation of Ambrok (ref. 5). When calculated by this method, the heat-transfer coefficient is multiplied by a factor of $(T_g/T_w)^{0.25}$ to account for the property variation across the boundary layer as suggested by Kays (ref. 6). For laminar boundary layers the gas side heat-transfer coefficient was based on the work of Brown and Donoughe (ref. 7) corrected for variable wall temperature by the results of Brown, Slone, and Richards (ref. 8). Transition from laminar flow was assumed to occur at the location which had a momentum thickness Reynolds number of 200 while the transition to turbulent flow was assumed to occur at the location which had a momentum thickness Reynolds number of 360. The thermal conductivity k_w in equation (2) was obtained from the table for MAR-M302 in reference 9.

Experimental impingement Nusselt numbers were obtained by evaluating equation (4) using both the experimental temperatures and an analytically predicted value for the gas side heat-transfer coefficient. These Nusselt numbers are plotted as a function of the experimental Reynolds number which is based on the jet flow and the nozzle diameter. An equal distribution of coolant flow to all of the holes in the impingement insert is assumed.

Predicted values of coolant side Nusselt numbers in the midchord region are obtained from correlations in the literature (refs. 10 to 17). These correlations apply to an average value of the Nusselt number for an array of jets impinging onto a flat plate. Appearing in table II is a list of these correlations.

RESULTS AND DISCUSSION

Wall Temperature Distribution

Experimental midspan temperature profiles for a range of midchord coolant- to gas-flow ratios are shown in figure 3. The coolant- to gas-flow ratios per vane varied from 0.0104 to 0.065 for the suction surface data of vane 2 and from 0.0094 to 0.063 for the pressure surface data of vane 3.

As shown in the figure, large nonlinear temperature gradients exist in the impingement cooled region. Because of these gradients, a two-dimensional heat-transfer analysis must be used to account for the chordwise conduction. Figures 1 and 3 show that there are three thermocouple locations on the suction and pressure surfaces which are included in the impingement cooled midchord region.

Heat-Transfer Coefficient Distribution

Two gas side heat-transfer coefficient distributions for the vane midspan are shown in figure 4. These two calculated profiles represent the two extremes in wall temperature profiles shown in figure 3; the higher heat-transfer coefficient is associated with the lower wall temperature. On the suction surface the momentum thickness Reynolds number criteria suggested laminar flow to an x/L of about 0.25. The impingement cooled region of the suction surface was in the transition regime. The flow on the pressure surface was considered to be turbulent.

Nusselt Number Correlation

Equation (4) was used to obtain experimental coolant side Nusselt numbers on the midchord suction and pressure surfaces. The value of h_g used in this equation was obtained by interpolating between the values of the maximum and minimum h_g 's in figure 4. The relative values of these h_g 's and, therefore, the relative Nusselt numbers, should be more accurate than the absolute values. The relative values are useful when considering the possible effect of crossflow on jet impingement heat transfer while the absolute values are useful when choosing an applicable correlation from the literature.

Crossflow effects. - Figure 5 is a comparison between the experimental and predicted coolant side Nusselt numbers at three thermocouple locations on both the suction and pressure surfaces. The comparison shows that the downstream locations have higher coolant side experimental Nusselt numbers than do the upstream locations. This is contrary to what would be normally expected if an adverse crossflow effect were present.

Crossflow effects are dependent on the ratio of the crossflow per unit area to jet flow per unit nozzle area. Usually, the smaller the value of this ratio, the smaller are the effects of crossflow on the heat-transfer characteristics of the impingement jet. This ratio can be expressed in the following way by assuming an equal flow to each of the impingement holes:

$$\frac{N\left(\frac{w_j}{A_{xf}}\right)}{\frac{w_j}{A_j}} = \frac{\frac{l}{X}\left(\frac{w_j}{zX}\right)}{\frac{w_j}{\frac{\pi d^2}{4} C_D}} = A_f \frac{l}{z} \quad (5)$$

Only a small amount of crossflow interference was encountered in reference 17 for values of $A_f(l/z)$ less than 0.2.

For the geometry of the vane herein, the quantity $A_f(l/z)$ is equal to or less than 0.34 and 0.23 for the suction and pressure surfaces, respectively, assuming an impingement hole discharge coefficient of 0.6. Calculations have shown that the downstream holes actually have 20 to 30 percent greater flow than the upstream holes. However, this unequal flow distribution cannot account for the upstream Nusselt numbers being small relative to the downstream Nusselt numbers as shown in figure 5. The higher downstream Nusselt numbers are probably due to a combination of impingement

cooling and some convection cooling from the crossflow. As a result of these data, the possibility of crossflow adversely affecting impinging jet heat transfer in a turbine vane seems minimal for the values of crossflow tested. A similar lack of crossflow effect for an impingement cooled turbine blade was observed in reference 1.

Correlation comparisons. - In figure 5(a), the data for the suction surface thermocouple location 5 compare favorably with the correlations from references 11, 13, and 17. The experimental Nusselt numbers for thermocouple locations 6 and 7 are 60 and 30 percent, respectively, of the experimental value at thermocouple location 5. In figure 5(b), the Nusselt numbers for the pressure surface thermocouple location 12 also compare favorably with the correlations of references 11, 13, and 17. The data for thermocouple locations 11 and 10 are approximately 65 and 45 percent, respectively, of the experimental values at thermocouple location 12.

Although some of the correlations are adequate for predicting the Nusselt numbers associated with thermocouple locations 5 and 12, none of the correlations are adequate for predicting the Nusselt numbers associated with thermocouple locations 6, 7, 10, and 11.

The data which appear in figure 5 have been reexpressed and now appear in figure 6. The characteristic length is the chordwise surface length between the thermocouple in question and the farthest upstream jet (see fig. 1). In the Reynolds number the mass flux is the local crossflow per unit crossflow area. As in figure 5, the data are separated into figure 6(a) for the suction surface and figure 6(b) for the pressure surface.

The data in figure 6 correlate independently of the thermocouple position as opposed to figure 5 in which the data correlate only for the individual thermocouple. Thus the existing methods of correlation which appear in the literature do not seem to be applicable for predicting data from an impingement cooled turbine vane having geometry similar to the one herein. The same can be said of the data for an impingement cooled blade discussed in reference 1.

SUMMARY OF RESULTS

The results of an investigation into the crossflow effects on impingement cooling the midchord region of a turbine vane are as follows:

1. Crossflow does not adversely affect the impingement cooling of the vane for the ratios of crossflow per unit area to jet flow per unit area less than 0.34.
2. Impingement cooling correlations found in the literature do not adequately predict the coolant side Nusselt numbers.

3. Impingement cooling Nusselt numbers were found to correlate with Reynolds numbers based on both crossflow and the distance between the point in question and the farthest upstream jet hole.

Lewis Research Center,
National Aeronautics and Space Administration,
Cleveland, Ohio, December 14, 1973,
501-24.

APPENDIX - SYMBOLS

A	area
A_f	ratio of effective jet area to cooled area
C_D	discharge coefficient
d	diameter of hole
E_1, E_2, E_3, E_4, E_5	constants in correlation equations in table II
G	mass velocity at nozzle exit
h	heat-transfer coefficient
k	thermal conductivity
L	chordwise surface length of vane
l	distance between impingement jet farthest upstream and point where cross-flow effect is to be evaluated
N	number of upstream spanwise rows of holes in impingement insert
Nu	Nusselt number
Pr	Prandtl number
Re	Reynolds number
T	temperature
t	thickness of wall
v	velocity
w	flow rate
X	center-to-center spacing in square array of adjacent jets
x	chordwise surface coordinate of vane
z	jet to plate spacing
μ	viscosity
ρ	density
Subscripts:	
a	arrival
c	coolant side
ci	coolant inlet

d based on hole diameter

g gas side

ge effective gas

i inside

j jet

n hole

o outside

s static

w wall

xf crossflow

xz surface distance between thermocouple and upstream end of impingement insert

REFERENCES

1. Gauntner, James W.; and Livingood, John N. B.: Engine Investigation of an Impingement Cooled Turbine Rotor Blade. NASA TM X-2791, 1973.
2. Calvert, Howard F.; Cochran, Reeves P.; Dengler, Robert P.; Hickel, Robert O.; and Norris, James W.: Turbine Cooling Research Facility. NASA TM X-1927, 1970.
3. Gladden, Herbert J.; Dengler, Robert P.; Evans, David G.; and Hippensteele, Steven A.: Aerodynamic Investigation of Four-Vane Cascade Designed for Turbine Cooling Studies. NASA TM X-1954, 1970.
4. Crowl, Robert J.; and Gladden, Herbert J.: Methods and Procedures for Evaluating, Forming, and Installing Small-Diameter Sheathed Thermocouple Wire and Sheathed Thermocouples. NASA TM X-2377, 1971.
5. Ambrok, G. S.: Approximate Solution of Equations for the Thermal Boundary Layer with Variations in Boundary Layer Structure. Soviet Phys. -Tech. Phys., vol. 2, no. 9, Sept. 1957, pp. 1979-1986.
6. Kays, W. M.: Convective Heat and Mass Transfer. McGraw-Hill Book Co., Inc., 1966.
7. Brown, W. Byron; and Donoughe, Patrick L.: Extension of Boundary Layer Heat Transfer Theory to Cooled Turbine Blades. NACA RM E50F02, Aug. 1950.
8. Brown, W. Byron; Slone, Henry O.; and Richards, Hadley T.: Procedure for Calculating Turbine Blade Temperatures and Comparison of Calculated with Observed Values for Two Stationary Air-Cooled Blades. NACA RM E52H07, Sept. 1952.
9. Anon.: High Temperature High Strength Nickel Base Alloys. The International Nickel Company, Inc., 2nd Ed., June 1968.
10. Kercher, D. M.; and Tabakoff, W.: Heat Transfer by a Square Array of Round Air Jets Impinging Perpendicular to a Flat Surface Including the Effect of Spent Air. Jour. Eng. Power, vol. 92, No. 1, Jan. 1970, pp. 73-82.
11. Kercher, D. M.: Heat Transfer by a Multiple Array of Round Jets Impinging Perpendicular to a Flat Surface Including Effects of Spent Air. M.S. Thesis, Univ. of Cincinnati, 1967.
12. Huang, G. C.: Investigations of Heat-Transfer Coefficients for Air Flow Through Round Jets Impinging Normal to a Heat-Transfer Surface. Jour. Heat Transfer, vol. 85, No. 3, Aug. 1963, pp. 237-245.

13. Walz, Dieter R. : Spot Cooling and Heating of Surfaces with High Velocity Impinging Air Jets. Part 2: Circular Jets on Plane and Curved Surfaces, Slot Jets on Curved Surfaces. Rep. TR-61, Stanford Univ. (AD-607727), July 1964.
14. Hilgeroth, E. : Heat Transfer in Jet Flow Perpendicular to the Transfer Surface. Chem. Ing. Tech., vol. 37, No. 12, Dec. 1965, pp. 1264-1272.
15. Ott, Hanns H. : Heat Transfer to a Plate Cooled by Air Flow. Schweiz. Bauzeitung, vol. 79, No. 46, Nov. 1961.
16. Gardon, Robert; and Cobonpue, John: Heat Transfer Between a Flat Plate and Jets of Air Impinging on It. International Developments in Heat Transfer. ASME, 1963, pp. 454-460.
17. Daane, R. A.; and Han, S. T. : An Analysis of Air-Impingement Drying. Tappi, vol. 44, No. 1, Jan. 1961, pp. 73-80.

TABLE I. - SURFACE DISTANCES OF THERMOCOUPLES
FROM VANE LEADING EDGE

Suction surface			Pressure surface		
Chordwise surface length of vane, L, cm (in.)					
7.27 (2.861)			6.53 (2.571)		
Thermocouple number	Location, x		Thermocouple number	Location, x	
	cm	in.		cm	in.
1	6.44	2.535	9	1.066	0.420
2	5.82	2.291	10	2.078	.818
3	5.34	2.102	11	2.782	1.095
4	4.685	1.845	12	3.57	1.405
5	3.875	1.526	13	4.343	1.710
6	2.98	1.173	14	4.92	1.937
7	2.304	.907	15	5.56	2.190
8	1.052	.414			

TABLE II. - CORRELATION EQUATIONS

Source	Correlation equation	Comment
Ref. 10, eq. (25)	$\frac{hd}{k} = E_1 E_2 \left(\frac{\rho v d}{\mu} \right)_n^{E_3} Pr^{1/3} \left(\frac{z}{d} \right)^{0.091}$	E_3 , E_1 , and E_2 are determined from figures 14, 16, and 17 of reference 10, respectively.
Ref. 11, eq. (7)	$\frac{\bar{h}X}{k} = 0.0364 \left(\frac{\rho v X}{\mu} \right)_n^{0.8} Pr^{1/3}$	-----
Ref. 12, figure 14	$\frac{\bar{h}d}{k} = E_4 \left(\frac{\rho v_a d}{\mu} \right)^{0.87} Pr^{1/3}$	E_4 is obtained from figure 14 of reference 12.
Ref. 13, eq. (20b)	$\frac{\bar{h}X}{k} = 0.0572 \left(\frac{GX}{\mu} \right)^{0.76} Pr^{1/3}$	-----
Ref. 14, eq. (11)	$\frac{\bar{h}X}{2k} = \frac{\left(9 - \frac{0.4X}{d} \right)}{100} \left(\frac{\rho v_n X}{2\mu} \right)^{0.75} \left(\frac{z}{d} \right)^{-0.2}$	-----
Ref. 15, eq. (14)	$\frac{\bar{h}d}{k} = 0.067 \left(\frac{\rho v_n d}{\mu} \right)^{0.74} Pr^{0.33} e^{(-0.061z/d)}$	-----
Ref. 16, eq. (2)	$\frac{\bar{h}X}{k} = 0.286 \left(\frac{\rho v_a X}{\mu} \right)^{0.625}$	-----
Ref. 17, figure 5	$\frac{\bar{h}d}{k} = E_5 \left(\frac{\rho v_n d}{\mu} \right)^{0.78} Pr^{1/3} C_D^{-0.11}$	E_5 is obtained from figure 5 of reference 17.

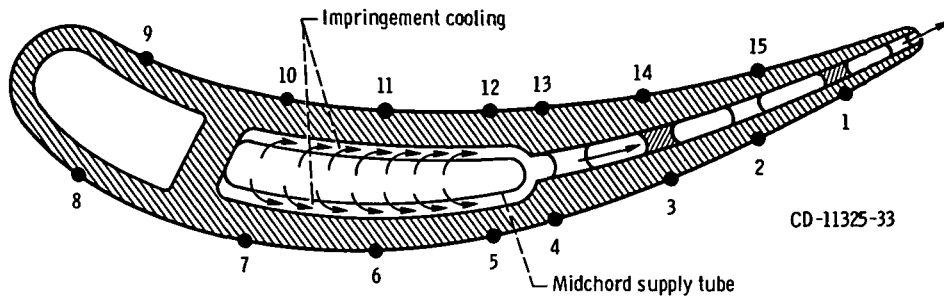


Figure 1. - Midspan cross-sectional schematic of test vanes showing composite location of thermocouples. (Numerals refer to thermocouple numbers.)

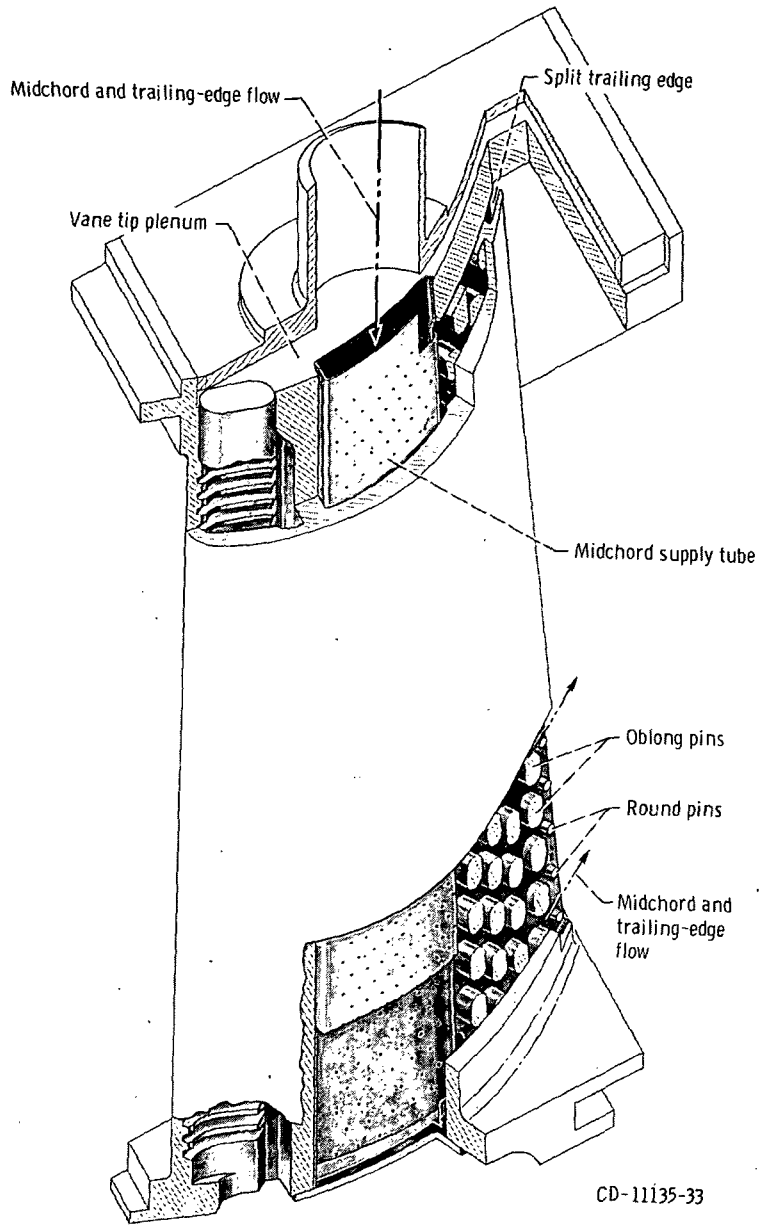


Figure 2. - Cutaway view of test vanes.

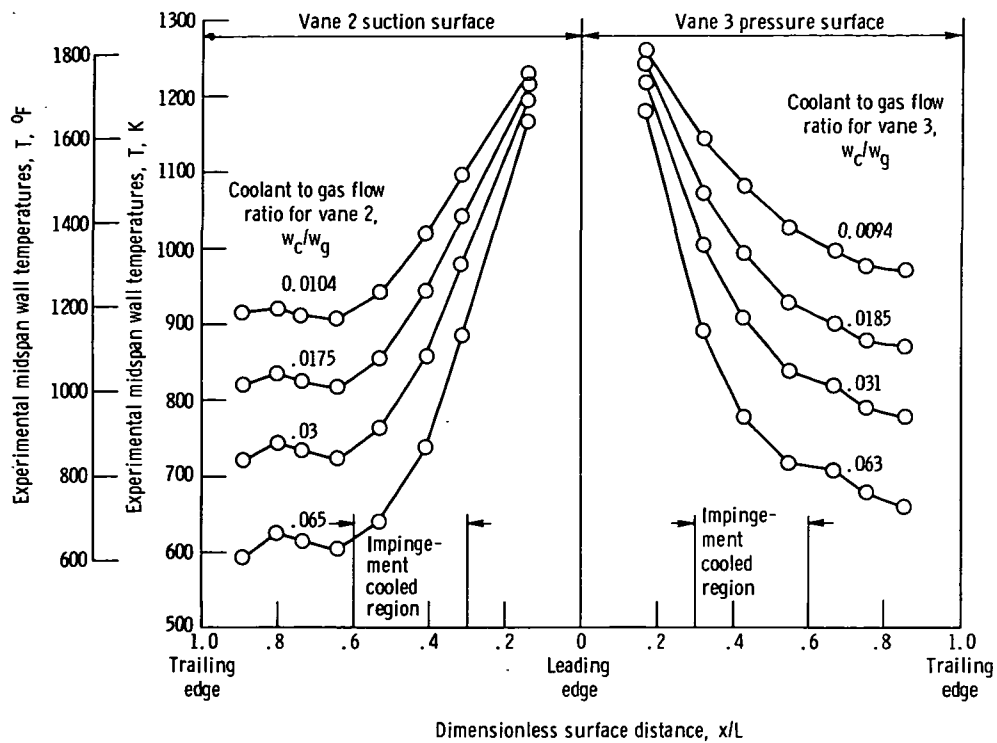


Figure 3. - Chordwise temperature, distribution of impingement cooled turbine vane for combustion gas temperature of 1255 K (1800° F) and coolant inlet temperature of 290 K (60° F).

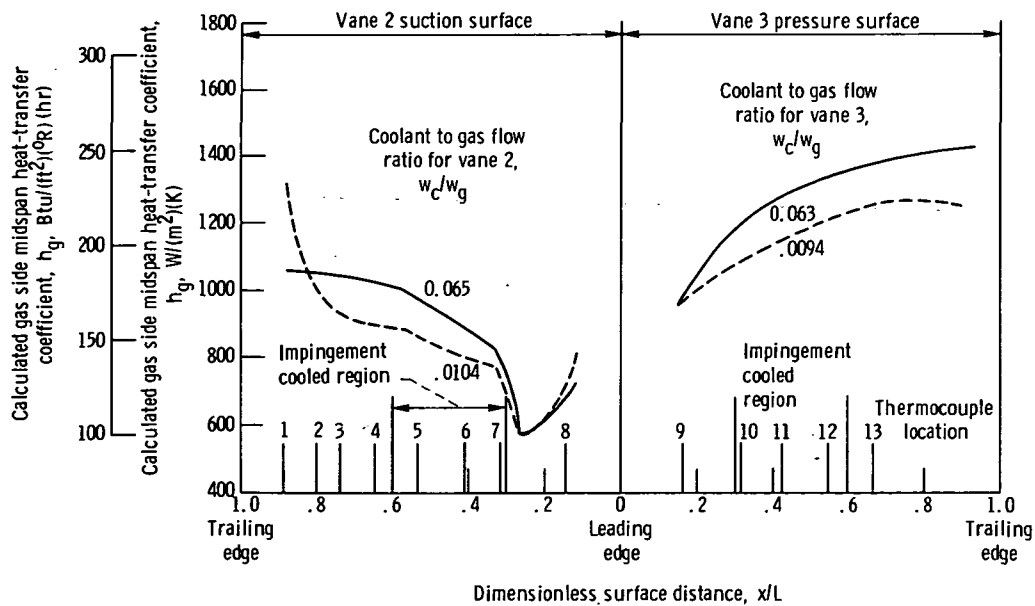


Figure 4. - Calculated gas side heat-transfer coefficient for impingement cooled turbine vane for combustion gas temperature of 1255 K (1800° F) and coolant inlet temperature of 290 K (60° F).

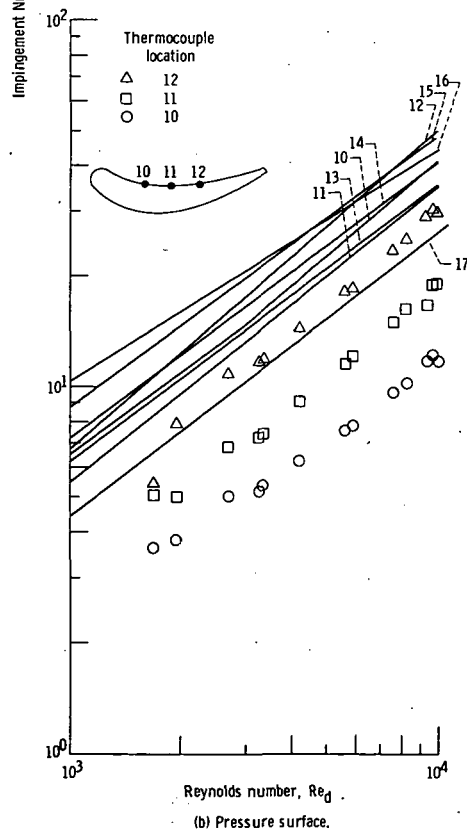
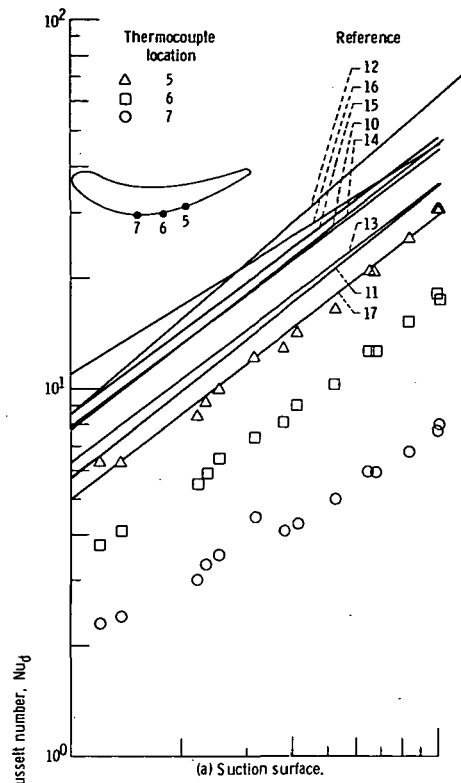


Figure 5. - Experimental and predicted coolant side Nusselt numbers as function of jet Reynolds number.

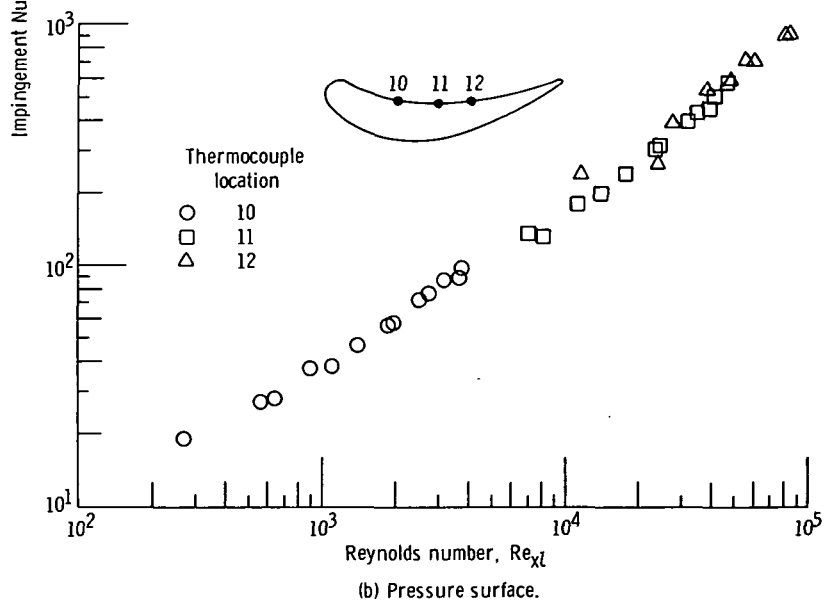
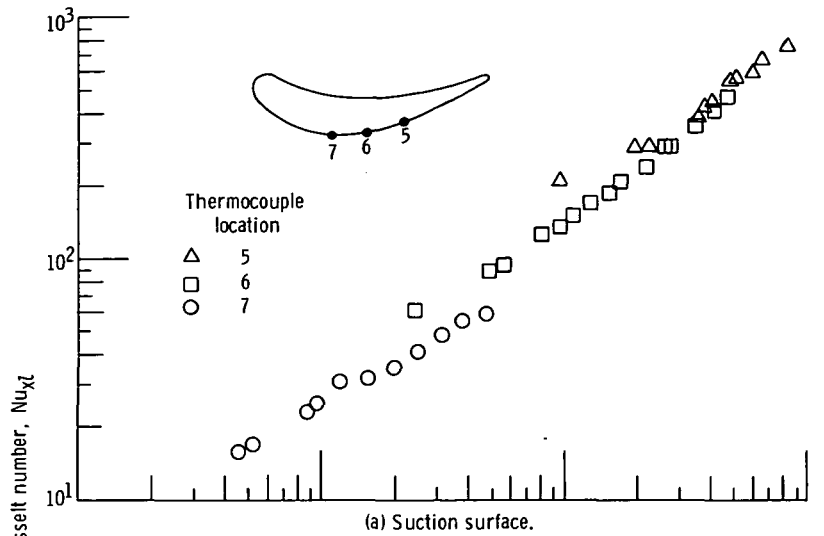


Figure 6. - Experimental coolant side Nusselt number as function of crossflow Reynolds number.



POSTMASTER : If Undeliverable (Section 158
Postal Manual) Do Not Return

"The aeronautical and space activities of the United States shall be conducted so as to contribute . . . to the expansion of human knowledge of phenomena in the atmosphere and space. The Administration shall provide for the widest practicable and appropriate dissemination of information concerning its activities and the results thereof."

—NATIONAL AERONAUTICS AND SPACE ACT OF 1958

NASA SCIENTIFIC AND TECHNICAL PUBLICATIONS

TECHNICAL REPORTS: Scientific and technical information considered important, complete, and a lasting contribution to existing knowledge.

TECHNICAL NOTES: Information less broad in scope but nevertheless of importance as a contribution to existing knowledge.

TECHNICAL MEMORANDUMS: Information receiving limited distribution because of preliminary data, security classification, or other reasons. Also includes conference proceedings with either limited or unlimited distribution.

CONTRACTOR REPORTS: Scientific and technical information generated under a NASA contract or grant and considered an important contribution to existing knowledge.

TECHNICAL TRANSLATIONS: Information published in a foreign language considered to merit NASA distribution in English.

SPECIAL PUBLICATIONS: Information derived from or of value to NASA activities. Publications include final reports of major projects, monographs, data compilations, handbooks, sourcebooks, and special bibliographies.

TECHNOLOGY UTILIZATION PUBLICATIONS: Information on technology used by NASA that may be of particular interest in commercial and other non-aerospace applications. Publications include Tech Briefs, Technology Utilization Reports and Technology Surveys.

Details on the availability of these publications may be obtained from:

SCIENTIFIC AND TECHNICAL INFORMATION OFFICE

NATIONAL AERONAUTICS AND SPACE ADMINISTRATION

Washington, D.C. 20546